



SPD_1495 Contributes to Capsular Polysaccharide Synthesis and Virulence in *Streptococcus pneumoniae*

Yun-Dan Zheng,^a Ying Pan,^a Ke He,^a Nan Li,^a Donghong Yang,^a Gao-Fei Du,^a Ruiguang Ge,^b Qing-Yu He,^a  Xuesong Sun^a

^aKey Laboratory of Functional Protein Research of Guangdong Higher Education Institutes, Institute of Life and Health Engineering, College of Life Science and Technology, Jinan University, Guangzhou, China

^bState Key Laboratory of Biocontrol, College of Life Sciences, Sun Yat-Sen University, Guangzhou, China

Yun-Dan Zheng, Ying Pan, and Ke He contributed equally to this article. Author order was determined by the importance of their work.

ABSTRACT *Streptococcus pneumoniae*, a Gram-positive human pathogen, causes a series of serious diseases in humans. SPD_1495 from *S. pneumoniae* is annotated as a hypothetical ABC sugar-binding protein in the NCBI database, but there are few reports on detailed biological functions of SPD_1495. To fully study the influence of SPD_1495 on bacterial virulence in *S. pneumoniae*, we constructed a deletion mutant (D39Δ*spd1495*) and an overexpressing strain (D39*spd1495*+). Comparative analysis of iTRAQ-based quantitative proteomic data of the wild-type D39 strain (D39-WT) and D39Δ*spd1495* showed that several differentially expressed proteins that participate in capsular polysaccharide synthesis, such as Cps2M, Cps2C, Cps2L, Cps2T, Cps2E, and Cps2D, were markedly upregulated in D39Δ*spd1495*. Subsequent transmission electron microscopy and uronic acid detection assay confirmed that capsular polysaccharide synthesis was enhanced in D39Δ*spd1495* compared to that in D39-WT. Moreover, knockout of *spd1495* resulted in increased capsular polysaccharide synthesis, as well as increased bacterial virulence, as confirmed by the animal study. Through a coimmunoprecipitation assay, surface plasmon resonance, and electrophoretic mobility shift assay, we found that SPD_1495 negatively regulated *cps* promoter expression by interacting with phosphorylated ComE, a negative transcriptional regulator for capsular polysaccharide formation. Overall, this study suggested that SPD_1495 negatively regulates capsular polysaccharide formation and thereby enhances bacterial virulence in the host. These findings also provide valuable insights into understanding the biology of this clinically important bacterium.

IMPORTANCE Capsular polysaccharide is a key factor underlying the virulence of *Streptococcus pneumoniae* in human diseases. Thus, a deep understanding of capsular polysaccharide synthesis is essential for uncovering the pathogenesis of *S. pneumoniae* infection. In this study, we show that protein SPD_1495 interacts with phosphorylated ComE to negatively regulate the formation of capsular polysaccharide. Deletion of *spd1495* increased capsular polysaccharide synthesis and thereby enhanced bacterial virulence. These findings further reveal the synthesis mechanism of capsular polysaccharide and provide new insight into the biology of this clinically important bacterium.

KEYWORDS *Streptococcus pneumoniae*, capsule, virulence

Streptococcus pneumoniae is a major pathogenic bacterium that causes various serious diseases in humans worldwide and may lead to high morbidity and mortality, especially among young children and elderly (1–3). The capsular polysaccharide (CPS) is recognized as one of the most important virulence factors of *S. pneumoniae* for infecting the host because nonencapsulated bacteria are almost completely harmless

Citation Zheng Y-D, Pan Y, He K, Li N, Yang D, Du G-F, Ge R, He Q-Y, Sun X. 2020. SPD_1495 contributes to capsular polysaccharide synthesis and virulence in *Streptococcus pneumoniae*. *mSystems* 5:e00025-20. <https://doi.org/10.1128/mSystems.00025-20>.

Editor Ileana M. Cristea, Princeton University

Copyright © 2020 Zheng et al. This is an open-access article distributed under the terms of the [Creative Commons Attribution 4.0 International license](https://creativecommons.org/licenses/by/4.0/).

Address correspondence to Ruiguang Ge, gerg@mail.sysu.edu.cn, Qing-Yu He, tqyhe@jnu.edu.cn, or Xuesong Sun, tsunxs@jnu.edu.cn.

Received 11 January 2020

Accepted 2 February 2020

Published 25 February 2020

(4–6). The ability to regulate CPS production is crucial for the survival of *S. pneumoniae* in different hosts.

CPS is required for effective colonization in the nasopharyngeal tract of the host and invasive infections in the blood and lungs (6, 7). First, to colonize the pharynx nasalis, *S. pneumoniae* reduces the synthesis of CPSs to increase the exposure of pneumococcal surface structures, such as adhesins, which are necessary for initial colonization. When *S. pneumoniae* escapes the nasopharynx, it invades the lungs and subsequently invades the bloodstream. During invasion, CPS is highly expressed to mask the surface antigens in order to reduce complement deposition and protect the bacterium against opsonophagocytosis (4, 8, 9).

Until now, more than 90 antigenically distinct serotypes of *S. pneumoniae* CPS have been identified, most CPSs are comprised of the repeating units such as glucose (Glu), L-rhamnose (Rha), L-rhamnose, L-rhamnose, glucose, and glucuronic acid (GlcUA), and all the CPSs, except for serotypes 3 and 37, are synthesized in the Wzx/Wzy-dependent pathway (6, 10–12). The *cps* gene cluster participated in the formation of CPS; it is located at the same region of the chromosome between the *dexB* and *aliA* genes, which encodes *cps2E*, *cps2D*, *cps2L*, *cps2I*, etc. (10, 13–15). Further, several possible transcriptional regulators of the *cps* locus, such as RegM (16), ComX (17), CopY (18), CpsR (19), GlnR (20), RitR (21), and ComE (9), have also been reported to regulate CPS formation. In particular, ComE exists in *S. pneumoniae* in nonphosphorylated and phosphorylated forms, and only the latter form can negatively regulate the expression of the *cps* gene cluster via interaction with the upstream promoter of *cps* *in vivo* (9).

Our group focused on the relationship between iron transportation and bacterial virulence. We found that in the $\Delta piuA \Delta piaA \Delta pitA$ triple mutant, in which three major iron transporters were simultaneously deleted, the protein SPD_1495 was evidently upregulated by 6.435- and 86.55-fold at the mRNA and protein levels, respectively, compared to that in D39-WT (22, 23). We speculated that SPD_1495 may also contribute to bacterial virulence. SPD_1495 is annotated as a sugar-binding protein in the NCBI database and is highly conserved in *Streptococcus* species. However, there are few reports on the detailed biological functions and the effects of SPD_1495 on bacterial virulence. Therefore, this study explores the biological function of SPD_1495 in *S. pneumoniae* using quantitative proteomics combined with biochemical validations. All of the experimental data indicated that SPD_1495 can interact with phosphorylated ComE to negatively regulate CPS formation. Our study provides novel insight regarding CPS formation, as well as the virulence ability of *S. pneumoniae*.

RESULTS AND DISCUSSION

Deletion of *spd1495* results in low utility of sugar source in *S. pneumoniae*. To elucidate the detailed biological function of SPD_1495 in *S. pneumoniae*, homologous replacement was used to obtain the deletion mutant D39 $\Delta spd1495$, and the plasmid pIB169-*spd1495* was transformed into D39-WT to construct the overexpression strain D39 $spd1495+$. Western blot analysis showed that the expression of SPD_1459 in D39 $spd1495+$ was significantly higher than that in D39-WT and that D39 $\Delta spd1495$ hardly expressed SPD_1495. These results indicated that the mutant strains were successfully constructed (Fig. 1A and B).

Since SPD_1495 is annotated as an ABC sugar-binding protein in the NCBI database, the utility of sugar source of D39-WT and D39 $\Delta spd1495$ was detected. Nutrition-restricted C+Y medium with or without a sugar source was used to obtain bacterial growth curves of the D39-WT and mutant strains (Fig. 1C). Without any sugar source in C+Y medium, the D39-WT, D39 $\Delta spd1495$, and D39-WT+*spd1495* strains almost did not grow. Therefore, *N*-acetylneuraminic acid (Neu5Ac), arabinose, xylose, glucose, fructose, lactose, sucrose, and maltose as the only sugar sources in C+Y medium promoted bacterial growth. The results showed that the addition of Neu5Ac, arabinose, and xylose as the only sugar sources in the culture medium almost rescued the growth of both the WT and mutant strains. The supplementation of glucose, fructose, lactose, sucrose, and maltose as the only sugar sources in C+Y medium can recover cell survival at different

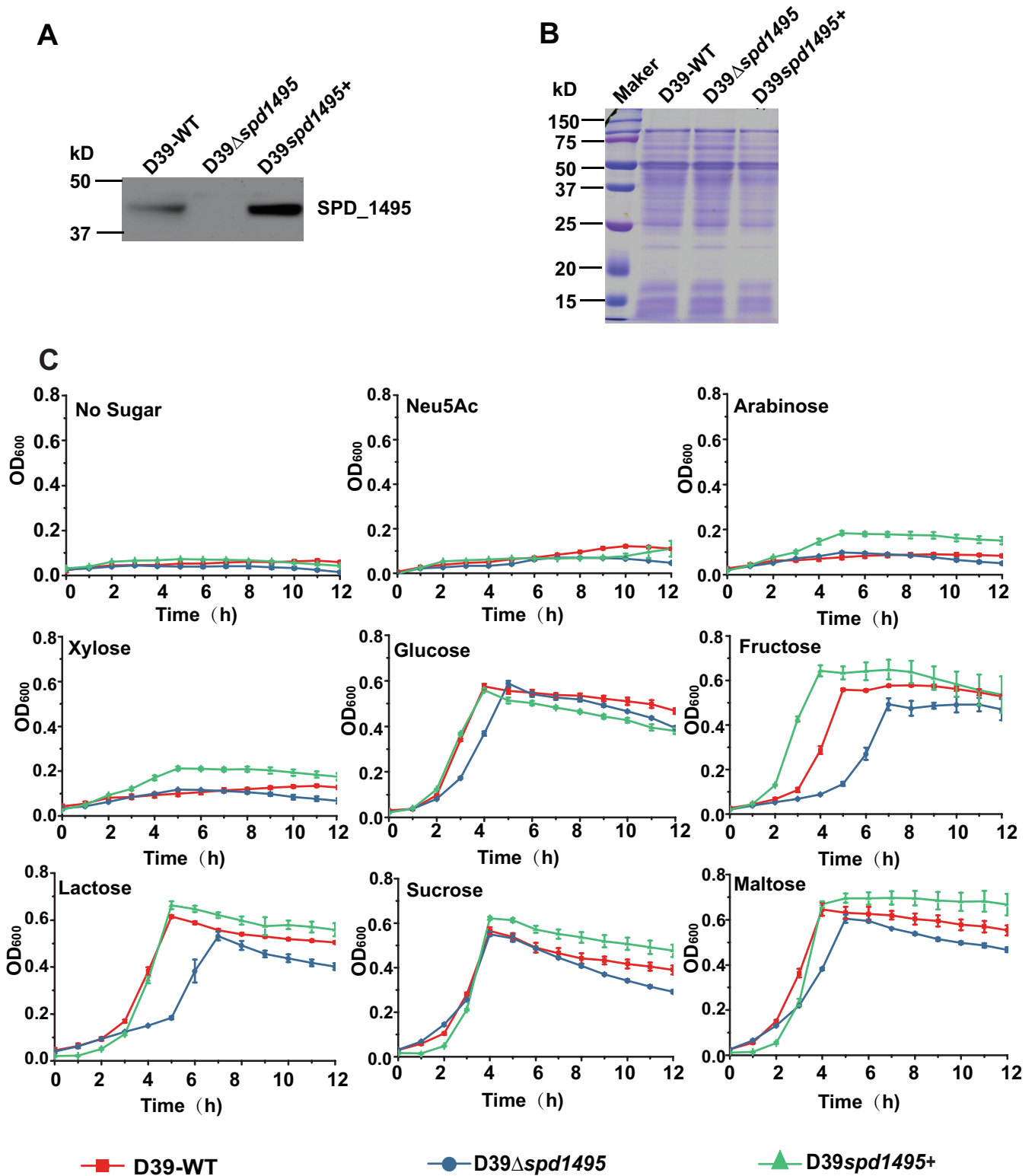


FIG 1 Deletion of *spd1495* affected the growth of *S. pneumoniae* D39 in medium containing different sugar sources. (A) Confirmation of gene deletion and overexpression of *spd1495* using Western blotting. (B) SDS-PAGE results of whole-cell lysates of D39-WT, D39 Δ spd1495, and D39spd1495+ strains as loading controls for the Western blotting experiments of panel A. (C) Growth curves of D39-WT (red), D39 Δ spd1495 (blue), and D39spd1495+ (green) strains cultured in C+Y medium containing no sugar, Neu5Ac, arabinose, xylose, glucose, fructose, lactose, sucrose, and maltose. Statistical analysis was conducted using Prism 6.0.

levels. Compared to that of D39-WT, D39 Δ *spd1495* showed obvious hysteresis of growth, especially when grown in C+Y medium supplemented with fructose and sucrose, whereas D39*spd1495*⁺ exhibited a marginal increase in growth. These results indicated that SPD_1495 may be a sugar-binding protein in *S. pneumoniae* and improve sugar utility of bacteria, which is consistent with the annotation in the NCBI database, but its detailed biological function was not reported.

Deletion of *spd1495* promotes the biosynthesis of CPS. To further explore the detailed biological function of SPD_1495 in *S. pneumoniae*, we used iTRAQ-based proteomics to identify differentially expressed proteins between D39-WT and D39 Δ *spd1495*. A strong correlation ($r^2 = 0.91374$) (Fig. 2A) indicated a good reliability with two independent biological replicates. A total of 994 proteins were commonly detected (Fig. 2B). More than 88% of the proteins had <50% variation (Fig. 2C), and the fold change threshold used to define differentially expressed proteins was <0.67 or >1.50 with $P < 0.05$. The relative quantitative analysis revealed 54 differentially expressed proteins in D39 Δ *spd1495*, with 34 upregulated and 20 downregulated proteins, compared to those in D39-WT (see Table S1 in the supplemental material).

KEGG (Kyoto Encyclopedia of Genes and Genomes) pathway enrichment analysis revealed that the differentially expressed proteins were enriched in three biological processes, namely, polyketide sugar unit biosynthesis, streptomycin biosynthesis, and acarbose and validamycin biosynthesis (Fig. 2D and E). It is noteworthy that the biosynthesis of polyketide sugar unit was the most significant pathway with the smallest P value among the three pathways. Following deletion of the *spd1495* gene, 34 proteins, including Cps2C, Cps2K, Cps2I, Cps2T, Cps2E and Cps2D etc., which are associated with CPS synthesis were obviously upregulated (Table 1). For example, Cps2L, Cps2M, Cps2N, Cps2T, Cps2F, Cps2G, Cps2I, and BgaA were involved in the synthesis of dTDP-L-rhamnose, a component in CPS synthesis (10). Furthermore, the STRING analysis (Fig. 2F and G) showed that the upregulated proteins in D39 Δ *spd1495*, such as Cps2C, Cps2K, Cps2I, Cps2T, Cps2E, and Cps2D, participate in the CPS synthesis network, and the raw materials, such as rhamnose, were used to promote CPS synthesis. The upregulation of *cps* gene was further validated by reverse transcription-quantitative PCR (RT-qPCR) analysis (Fig. 3A). Moreover, we also found that many upregulated proteins in D39 Δ *spd1495*, such as LacB, LacD, DexB, BglA-1, SPD_0559, SPD_1664, and SPD_0412, formed a small network. These proteins are involved in carbohydrate metabolism, which supplies some of the key raw materials for CPS synthesis, such as ATP and NAD⁺/NADPH, etc. (24). The 20 downregulated proteins were not enriched into any biological progress. Thus, both KEGG pathway enrichment analysis and STRING analysis indicated that the upregulated proteins are enriched in CPS synthesis. Therefore, we speculated that CPS synthesis in *S. pneumoniae* is negatively regulated by SPD_1495.

To validate the relationship between the CPS synthesis and SPD_1495 in *S. pneumoniae*, transmission electron microscopy (TEM) was used to detect the thickness of the CPS. The images of TEM showed that the thickness of CPS decreased in the following order: D39 Δ *spd1495* > D39-WT > D39*spd1495*⁺. This indicates that SPD_1495 could negatively regulate CPS formation (Fig. 3B). The relative content of uronic acid, which is the main component of the capsule, was determined to further quantitatively compare the difference in CPS formation. As shown in Fig. 3C, the content of uronic acid decreased in the following order: D39 Δ *spd1495* > D39-WT > D39*spd1495*⁺; this is consistent with the order of decrease in capsule thickness. Therefore, both the thickness of CPS and the content of uronic acid confirmed that, compared to the D39-WT, D39 Δ *spd1495* produced higher quantities of CPS. These results jointly indicated that SPD_1495 negatively regulated capsule formation.

Deletion of *spd495* increases virulence in *S. pneumoniae*. The CPS plays an important role in the virulence of *S. pneumoniae* (25). The survival rates of mice infected with D39-WT, D39 Δ *spd1495*, and D39*spd1495*⁺ were determined to uncover the contribution of SPD_1495 to bacterial virulence. As shown in Fig. 3D, the D39 Δ *spd1495*

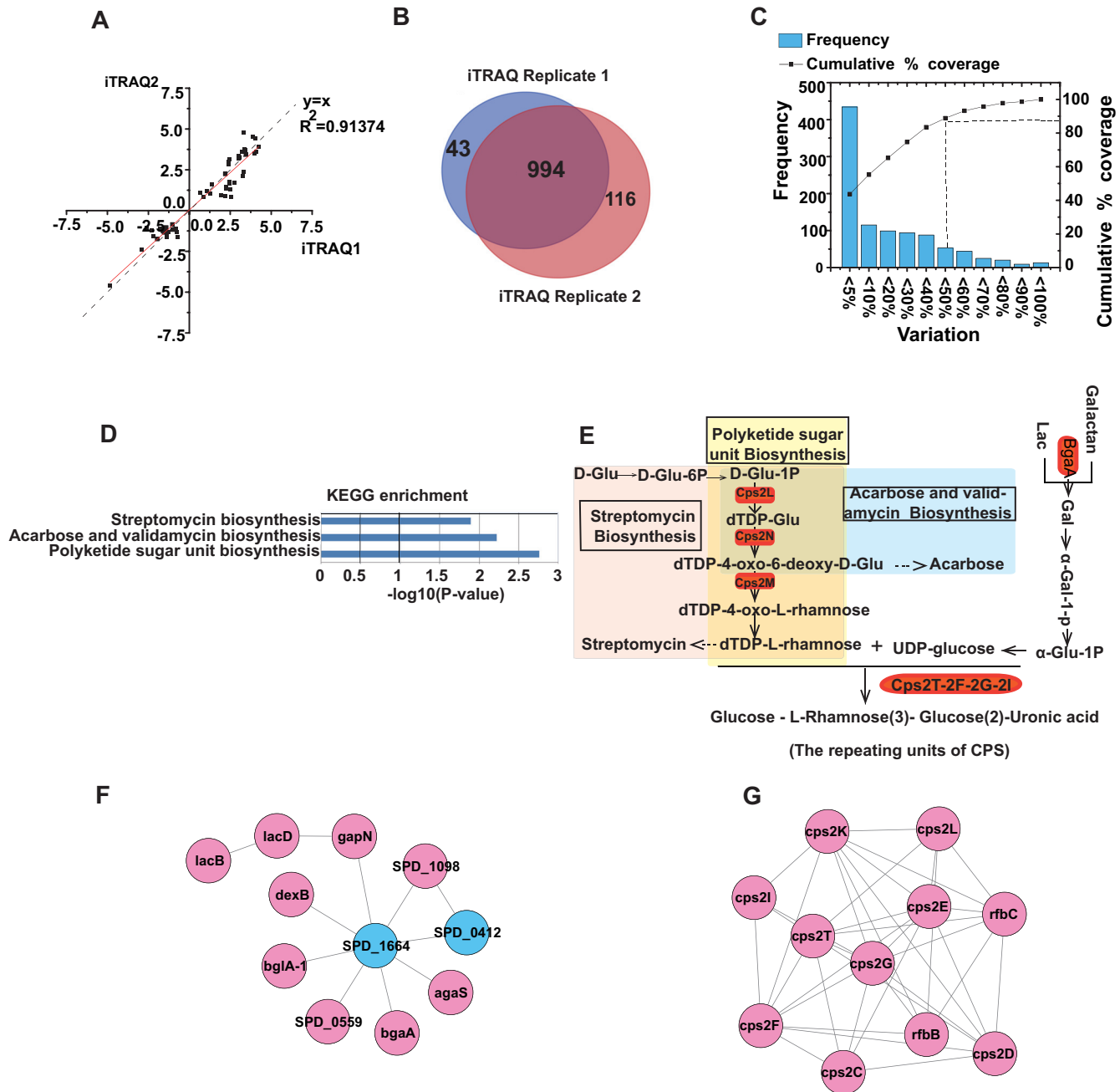


FIG 2 Results of iTRAQ-based proteomics quantitative analysis. (A) Correlation of the fold change in differential proteins in two replicates. (B) The number of total proteins was identified in two biological replicates. (C) Distribution of biological variables in two replicates. (D) KEGG pathway enrichment analysis of differentially expressed proteins. (E) The pathways of polyketide sugar unit biosynthesis, streptomycin biosynthesis, and carbose and validamycin biosynthesis were enriched by KEGG. (F) Differentially expressed proteins involved in sugar metabolism network. (G) Differentially expressed proteins involved in the CPS synthesis network. Red represents upregulated proteins, whereas blue represents downregulated proteins.

mutant was more virulent than D39-WT; however, the virulence of SPD_1495-overexpressing strains was very similar to that of D39-WT in the mouse pneumonia model. This result indicated that SPD_1495 may increase the virulence of *S. pneumoniae* by decreasing the formation of the CPS and demonstrated that SPD_1495 affects the pathogenicity of *S. pneumoniae* during infection *in vivo*.

SPD_1495 affects the formation of *S. pneumoniae* CPS via interacting with phosphorylated ComE. In order to seek regulation network of SPD_1495, the SPD_1495 was expressed and purified by glutathione *S*-transferase (GST) tag affinity chromatography.

TABLE 1 Some differently expressed proteins in D39 Δ *spd1495* compared to D39-WT

Gene or protein	Protein	Avg fold change	Avg $-\log_{10} P$
Carbohydrate metabolic process			
<i>bgaA</i>	β -Galactosidase, putative	4.30	9.80
<i>bglA-1</i>	6-Phospho- β -glucosidase	7.55	4.89
<i>dexB</i>	Glucan 1,6- α -glucosidase	19.24	4.24
<i>lacD</i>	Tagatose 1,6-diphosphate aldolase	2.89	3.48
<i>lacB</i>	Galactose-6-phosphate isomerase	3.82	1.88
Capsule-associated proteins			
Cps2L	Glucose-1-phosphate thymidyltransferase	10.86	6.94
Cps2K	Cps2K	14.65	0
Cps2C	Polysaccharide export protein	9.18	4.85
Cps2D	Cps2D	4.66	1.50
Cps2F	Glycosyl transferase, group 2 family protein	10.87	5.70
Cps2G	Glycosyl transferase, group 1 family protein	8.57	2.50
Cps2M	Cps2M	11.96	2.27
Cps2I	Cps2I	7.14	2.26
Cps2T	Cps2T	11.92	6.56
Cps2E	Cps2E	6.15	2.19
Cps2N	dTDP-glucose 4,6-dehydratase	17.01	7.51

There was a band of ~ 45 kDa, corresponding to the calculated molecular weight of SPD_1495 in SDS-PAGE, the Western blotting with SPD_1495 antibody confirmed the expression of SPD_1495 (Fig. 4A and B). The proteomic data and detection of capsule showed that the formation of CPS was negatively regulated by SPD_1495. In *S. pneumoniae*, the *cps* gene cluster is mainly responsible for the CPS biosynthesis (19). We speculated that SPD_1495 may regulate the expression of the *cps* gene cluster via interaction with the CPS operon. However, electrophoretic mobility shift assay (EMSA) results revealed that

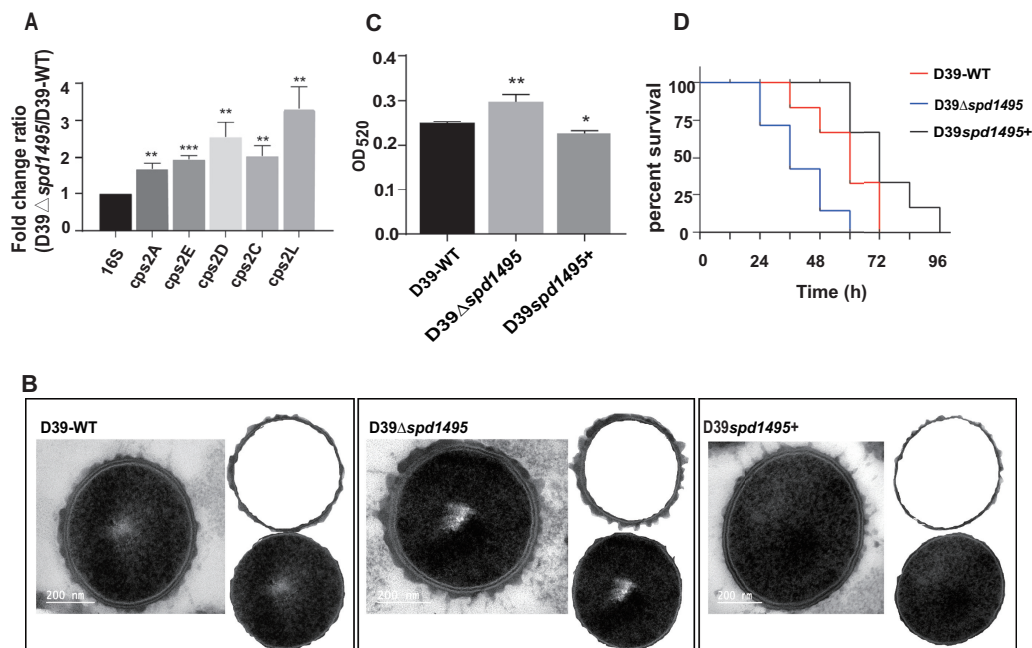


FIG 3 SPD_1495 negatively regulated capsular synthesis. (A) SPD_1495 negative regulate the *cps* genes expression in D39-WT and D39 Δ *spd1495*. (B) TEM results for strains D39-WT, D39 Δ *spd1495*, and D39*spd1495*⁺. (C) Uronic acid contents in strains D39-WT, D39 Δ *spd1495*, and D39*spd1495*⁺. (D) The virulence of strains D39-WT, D39 Δ *spd1495*, and D39*spd1495*⁺. Data were analyzed by two-tailed, unpaired Student *t* tests, and results are expressed as means \pm the SD. ***, $P < 0.001$; **, $P < 0.01$; *, $P < 0.05$.

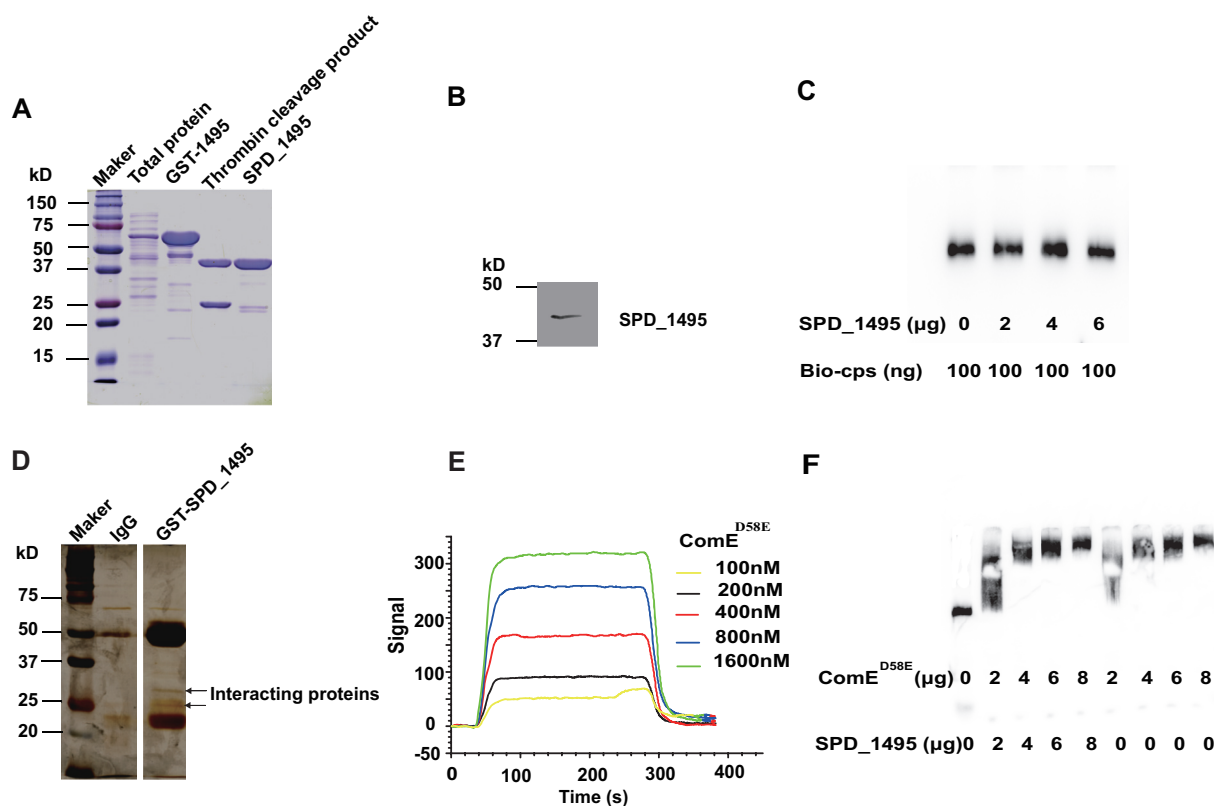


FIG 4 SPD_1495 interacted with ComE. (A) SDS-PAGE results of SPD_1495 expression, visualized using a PGEX-4T-1 fusion system and purified by GST affinity column. (B) Western blotting assay of SPD_1495 expression using anti-SPD_1495 antibody. (C) EMSA with SPD_1495 cannot bind to Bio-*cps* probe. (D) The potential proteins interacting with SPD_1495 were screened by a Co-IP assay and are indicated by arrows. (E) SPR detected the interaction of ComE^{D58E} with SPD_1495. (F) EMSA demonstrated that ComE^{D58E}, the complexes of ComE^{D58E}, and SPD_1495 bind to the Bio-*cps* probe.

SPD_1495 cannot directly interact with *cps* operon (Fig. 4C). A previous study by Zheng et al. identified the transcriptional regulator in the upstream promoter region of *cps* by DNA-pull-down but did not find SPD_1495 (9). Therefore, we deduce that SPD_1495 may negatively regulate CPS formation indirectly.

A coimmunoprecipitation (Co-IP) assay was performed to identify the proteins interacting with SPD_1495. Compared to that of IgG in the control group, SPD_1495 specifically captured some proteins of molecular weight between 20 and 37 kDa (Fig. 4D). These proteins were cut and digested with trypsin and then were identified by mass spectrometry. The identification results showed that SPD_1495 can interact with several proteins, including RpsC, ComE, SPD_1495, RecA, CshB, and CoaC (Table 2). Notably, ComE exists in two forms (nonphosphorylated and phosphorylated) in *S. pneumoniae*, and only phosphorylated form ComE negatively regulates the expression of the *cps* gene cluster via an interaction with the upstream promoter of *cps* (9). Thus, to further uncover the function of SPD_1495 in the formation of CPS, a phosphomimetic form (ComE^{D58E}) was expressed and purified to check its interaction with

TABLE 2 Proteins interacting with of SPD_1495 identified in a Co-IP assay

Protein	Function	Coverage (%)
RpsC	30S ribosomal protein S3	73.7
ComE	Response regulator	50.4
SPD_1495	Sugar ABC transporter, sugar-binding protein	58.8
RecA	Protein RecA	54.6
CshB	DEAD-box ATP-dependent RNA helicase CshB	58.8
CoaC	Phosphopantothencycysteine decarboxylase	53.6

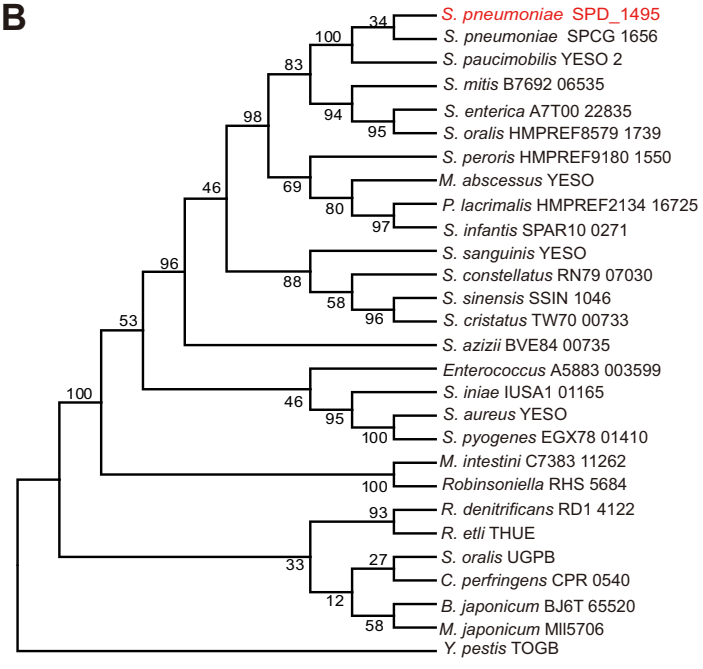
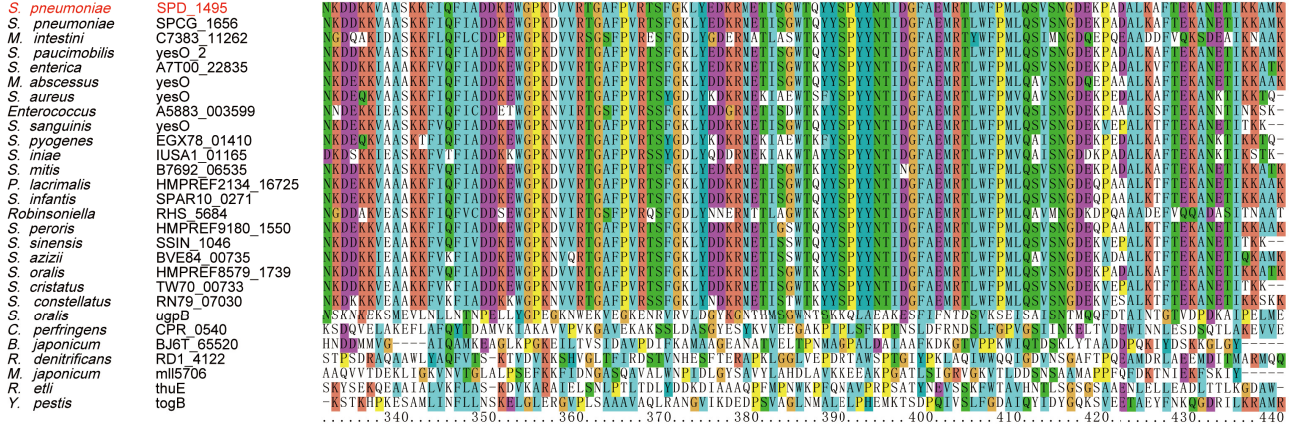
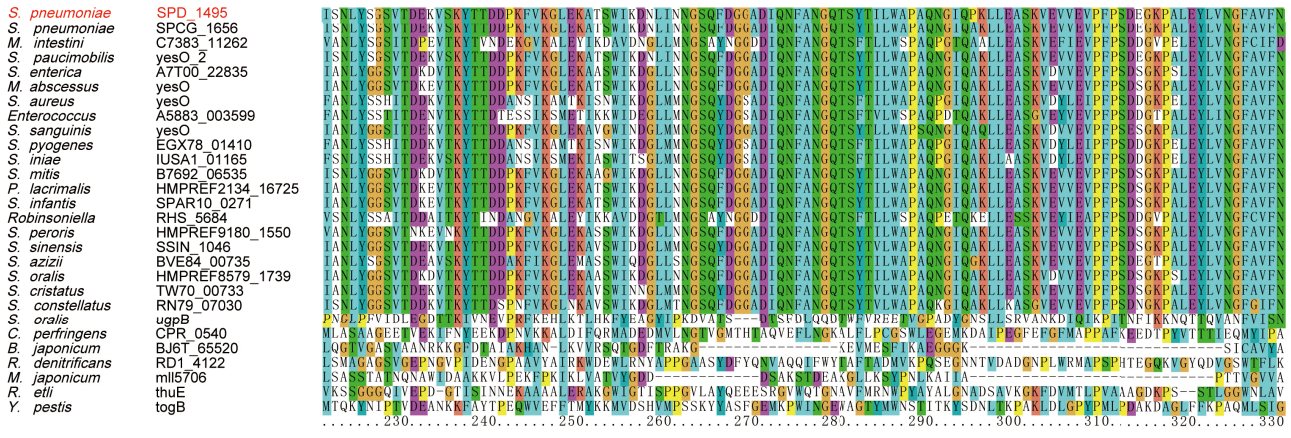


FIG 5 (Continued)

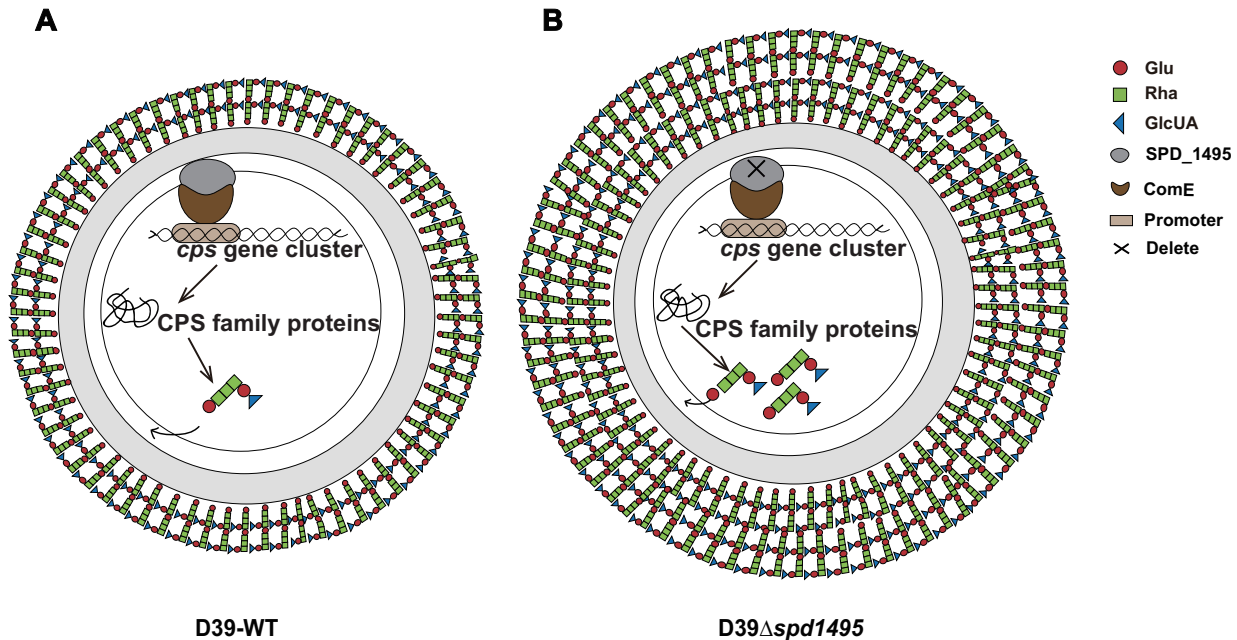


FIG 6 Integrated model of SPD_1495 function in *S. pneumoniae* in this study. (A) In D39-WT, SPD_1495 interacted with ComE to negatively regulate capsular polysaccharide synthesis, resulting in normal capsule thickness. (B) In D39 Δ *spd1495*, without interaction between SPD_1495 and ComE, the bacterial capsule became thickened.

function of SPD_1495 in *S. pneumoniae* CPS synthesis. Hence, the regulation of capsule formation and bacterial virulence of SPD_1495 observed in the present study may represent a novel biological function of this cluster of proteins.

Previous research has shown that the CPS of *S. pneumoniae* is one of the key virulence factors required for effective infection host (26, 27), and many vaccines targeting CPS have been developed to treat or prevent bacterial infections in recent years (28). In this work, convincing evidence was obtained indicating that SPD_1495 can negatively regulate CPS synthesis by interacting with phosphorylated ComE in *S. pneumoniae*. Further, SPD_1495 is highly conserved among Gram-positive bacteria. Our data suggest that SPD_1495 is a vaccine or drug target candidate because of its contribution to virulence during bacteremia. Accordingly, our further studies will investigate whether SPD_1495 can be an efficacious vaccine antigen for preventing *S. pneumoniae* infection.

Conclusion. Taken together, our research revealed the biological function of SPD_1495 in capsule formation in *S. pneumoniae*. This protein negatively regulates CPS synthesis by interacting with phosphorylated ComE, a key transcriptional regulator located in the *cps* locus. Thus, deletion of the *spd1495* gene will increase the production of dTDP-L-rhamnose, thereby promoting the biosynthesis of CPS. Furthermore, the CPS is recognized as one of the most important virulence factors in *S. pneumoniae* for infecting the host. deletion of *spd1495* will upregulates the CPS to improve the virulence factor related to the host, thereby enhancing the ability of *S. pneumoniae* to infect host cells (Fig. 6). Considering the importance of CPS in bacterial adherence and entry into the host, regulation of SPD_1495 is essential in *Streptococcus* infection. Moreover, the animal assay indicated that SPD_1495 is an important protein in regulating the virulence in *S. pneumoniae*. Therefore, SPD_1495 may be a vaccine or drug target candidate for the development of novel antibacterial to treat the *Streptococcus* infections.

MATERIALS AND METHODS

Bacterial growth conditions. The *S. pneumoniae* D39 was cultured in THY medium (Todd-Hewitt broth; Oxoid, UK) with 0.5% yeast extract (Oxoid) or on Columbia agar (Difco, USA) containing 5% sheep

TABLE 3 Bacterial strains and plasmids used in this study

Strain or plasmid	Relevant characteristic(s) ^a	Source or reference
Strains		
<i>S. pneumoniae</i>		
D39	Wild type	ATCC (USA)
Δ <i>spd1495</i> mutant	In-frame <i>spd1495</i> mutant strain derived from D39; Erm ^r	This study
D39/pIB169- <i>spd1495</i>	D39 strain transformed with pIB169- <i>spd1495</i> ; Cm ^r	This study
<i>E. coli</i>		
BL21	Wild type	Invitrogen (USA)
BL21/pGEX-4T-1- <i>spd1495</i>	BL21 strain transformed with pGEX-4T-1- <i>spd1495</i> ; Amp ^r	This study
Plasmids		
pGEX-4T-1	pGEX vector contained <i>tac</i> promoter; Amp ^r	Invitrogen (USA)
pGEX-4T-1- <i>spd1495</i>	<i>S. pneumoniae</i> D39 <i>spd1495</i> (33–442 AA) fragment cloned into pGEX-4T-1; Amp ^r	This study
pIB169	Shuttle plasmid contained P _{veg} promoter; Cm ^r	14
pIB169- <i>spd1495</i>	<i>S. pneumoniae</i> D39 <i>spd1495</i> (1–442 AA) fragment cloned into pIB169; Cm ^r	This study
pET-28b(+)	pET-28b(+) vector contained T7 promoter; Kan ^r	Novagen (USA)
pET-28b(+)- <i>comE</i> ^{D58E}	<i>S. pneumoniae</i> D39 <i>comE</i> (1–250 AA) fragment cloned into pIB169; Cm ^r	This study

^aErm^r, erythromycin resistance; Cm^r, chloramphenicol resistance; Amp^r, ampicillin resistance. Kan^r, kanamycin resistance; AA, amino acids.

blood (Ruite, China) at 37°C in a 5% CO₂ incubator (MCO-170AICUVHL-PC; Panasonic, Japan). *Escherichia coli* DH5 α and BL21 (Invitrogen, USA) were both cultured in Luria-Bertani (LB) medium at 37°C in an incubator shaker (Yi Heng, China). All strains were stored at –80°C in 15% glycerol. Erythromycin (Erm; Sigma, USA) at 0.25 mg/ml, chloramphenicol (Cm; Sigma) at 4 mg/ml, or ampicillin (Amp; Sigma) at 100 μ g/ml was added to the medium when needed for selective culture. All of the bacterial strains and plasmids used are listed in Table 3.

Construction of mutant *S. pneumoniae* D39 strains. Long-flanking-homology PCR (LFH-PCR) was used to construct strain D39 Δ *spd1495* (29, 30), and the primers used in this study are listed in Table 4. The target gene, *spd1495* (1,329 bp), was replaced by an antibiotic resistance cassette gene (*erm*). The reconstructed region, including *erm* (829 bp), upstream (817 bp) and downstream (624 bp) of *spd1495* was ligated by LFH-PCR using primers P3 to P8. The products of LFH-PCR were transferred into strain D39-WT, and the positive transformant was selected by Erm-containing Columbia sheep blood agar plate. D39 Δ *spd1495* strains were stocked after seven sequential passages in the THY medium with 0.25 μ g/ml Erm. To construct *spd1495*-overexpressing strains, the recombinant plasmid pIB169-*spd1495* was constructed by inserting the *spd1495* gene (1,329 bp) into pIB169 plasmid using a ClonExpress II

TABLE 4 Primers used in this study

Primer	Sequence (5'–3')
P1(<i>spd1495</i> -F)	GATCTGGTCCCGGTGGATCCTCAGGTGGTGACGGTGCCAAAACAG
P2(<i>spd1495</i> -R)	TCAGTCAGTCACGATCGCGCCGCTATTGTTTCATAGCTTTTTTTG
P3(<i>spd1495</i> -up-F)	GCCTGTTTAGCGATGTACCATAGTG
P4(<i>spd1495</i> -up-R)	ATTCTATGAGTCGCTGCCGACTTCTTAGTATTCTATAAAAAGT
P5(<i>erm</i> -F)	AGTCGGCAGCGACTCATAGAAT
P6(<i>erm</i> -R)	CCGGCCCAAATTTGTTTGGAT
P7(<i>spd1495</i> -down-F)	ATCAAACAATTTTGGGCCGGTGTATTCTCTATGAATAAGC
P8(<i>spd1495</i> -down-R)	GTGGGTATAAATCCATTTCCAAC
P9(pIB169- <i>spd1495</i> -F)	GGAGACCGCGTCCGAATTCATGAAATTTAGAAAATTAGCTGTACAGTAC
P10(pIB169- <i>spd1495</i> -R)	GGTGCACCTCGAGGGATCCGTGATGGTGATGGTGATGTTGTTTCATAGCTTTTTTATTG
P11(ComE-F)	GGATCTTCCAGAGATGGATCCATGAAAGTTTTAATTTAGAAAGATGTTATTGA
P12(ComE-R)	CTGCCGTTCCGACGATCTCGAGTCACTTTTGAGATTTTTCTCTAAAATATC
P13(ComE ^{D58E} -R)	TTATTTCTAGAAATCGATATTCATGGAATTGA
P14(ComE ^{D58E} -F)	GAATATCGATTTCTAGGAAATAAAGCTGATTTA
P15 cpsF Bio-	TACACATCTGCTTCTAAAATATTGT (labeled by biotin)
P16 cpsR	TTAAAACGTCTACTCATGATTAACA
P17 cps2A-F	TAGCCGATGGAGACCGTGAC
P18 cps2A-R	TCTGGCATTGCATAAGAAGGAAG
P19 cps 2C-F	ACGACTCCTTCTTCCAAATGTT
P20 cps 2C-R	CAAATCTGGAACGAGCCCTAAA
P21 cps 2D-F	ACCGAATCCGACAGCTTCT
P22 cps 2D-R	TCACCTGCCTCCGTCACATAAA
P23 cps 2E-F	TTGTTGGGGAGTTGGTAGCCG
P24 cps 2E-R	TGCCATCTCACGAATTTGCTT
P25 cps 2L-F	GATAGCGTTGCTTTAATCTTGGG
P26 cps 2L-R	GGAGCGAGGACACTCTGGTTTT
P2716S rRNA-F	CTGCGTTGTATTAGCTAGTTGGTG
P2816S rRNA-R	TCCGTCCATTGCCGAAGATTC

one-step cloning kit (Vazyme, China). The recombinant plasmid pB169-*spd1495* containing an Cm resistance cassette was then transferred into the D39-WT strain. The transformants were screened in Cm-containing Columbia sheep blood agar plate. Finally, all of the mutant strains, including D39 Δ *spd1495* and D39*spd1495*⁺, were confirmed by Western blotting (31).

Cloning, expression, and purification of SPD_1495 and ComE^{D58E}. The *spd1495* gene was amplified from *S. pneumoniae* D39 genomic DNA (the primers are listed in Table 4). The product of PCR and pGEX-4T-1 plasmid were digested by restriction enzymes BamHI and Not I (TaKaRa, Japan), and then the digested fragments were ligated by the ClonExpress II kit. The constructed plasmid pGEX-4T-1-*spd1495* was verified by sequencing (Sangon Biotech, China) and then transferred into *E. coli* BL21. For SPD_1495 expression, BL21/pGEX-4T-1-*spd1495* was cultured in LB medium with 100 μ g/ml Amp in a shaking incubator at 37°C. When the optical density at 600 nm (OD₆₀₀) reached 0.6 to 0.8, protein expression was induced by adding 0.5 mM isopropyl- β -D-thiogalactopyranoside (IPTG; Sigma) with a further 5 h of incubation. The bacteria were harvested by centrifugation at 8,000 \times *g* for 10 min at 4°C and washed with 0.01 M phosphate-buffered saline (PBS) three times. The harvested cells were suspended in 0.01 M PBS and lysed by sonication. GST-SPD_1495 fusion protein was isolated by glutathione-Sepharose 4B (GE Healthcare Life Science, Sweden) and digested with thrombin in 0.01 M PBS buffer according to the manufacturer's instructions to remove the GST tag. The purified SPD_1495 was then used as an antigen for antibody preparation (Tianjin Sun gene Biotech Co., China). The BALB/c mice (6 to 8 weeks old, weighing ~20 g) were immunized with 100 μ g of GST-SPD_1495 by subcutaneous injections. After 2 weeks, secondary immunization was performed. A booster dose was administered intravenously to enhance immunity. The spleen cells of the immunized mice were then fused with hybridoma cells and diluted in Dulbecco modified Eagle medium. Hybridomas were tested by indirect enzyme-linked immunosorbent assay (Cusabio, China). The isotype of each monoclonal antibody (MAb) was determined. Ascites were produced in BALB/c mice, and then MAbs were purified and biotinylated (32). A phosphomimetic mutant, ComE^{D58E}, was constructed by site-directed mutagenesis of *comE* to exhibit the activity of ComE protein *in vitro*. Both wild-type ComE and ComE^{D58E} were expressed and purified as described previously (9, 33, 34). The primers are listed in Table 4 (ComE-F to 16S rRNA-R).

Western blot assay. From each sample, 25 μ g of protein was loaded into 12% SDS-PAGE gels and then transferred onto a polyvinylidene fluoride (polyvinylidene difluoride) membrane (Millipore, USA). Anti-SPD_1495 antibody was incubated with polyvinylidene difluoride membrane at 4°C, and horseradish peroxidase-conjugated goat anti-mouse was used as a secondary antibody. The results were visualized with Clarity Western ECL Substrate (Bio-Rad, USA) and captured using ImageMaster 2D Platinum 6.0 (GE Healthcare, USA). Meanwhile, SDS-PAGE gels stained with Coomassie brilliant blue G250 were used as a loading control.

Growth curve analysis. The D39-WT and mutant strains were cultured in C+Y medium (no sugar) with Neu5Ac, arabinose, xylose, glucose, fructose, lactose, sucrose, and maltose as only sugar source, respectively, at equivalent inoculation doses at 37°C in a 5% CO₂ incubator. The OD₆₀₀ was continuously measured every hour by UV-visible spectroscopy (Evolution 300; Thermo Fisher Scientific, USA) for 12 h, and the data were analyzed by Prism 6.0 (GraphPad Software, USA).

Protein preparation, iTRAQ labeling, and proteomics analysis. From each sample, 200 μ g of protein was extracted from D39-WT and D39 Δ *spd1495* strains in the exponential growth phase, digested with trypsin (Promega, USA) at 37°C for 16 h, and lyophilized. Then, a iTRAQ reagent multiplex kit (AB Sciex, USA) was used to label peptide samples according to the manufacturer's protocol. D39-WT and D39 Δ *spd1495* strains were labeled with 114 and 116 isobaric tags for 1 h at room temperature, respectively. The labeled peptides from the two groups were mixed in equal proportions and dried. High-performance liquid chromatography (WuFeng, China) with a TechMate C18-ST column (4.6 mm \times 250 mm, 5 μ m; TechMate, China) was used to separate the labeled peptides. In brief, an iTRAQ-labeled peptide mixture was eluted with a gradient of 2 to 80% acetonitrile in 20 mM ammonium formate (pH 10.0) for 65 min at a flow rate of 0.8 ml/min. The peptide elution was monitored at 214 nm. The eluted peptides were collected every minute, pooled into six fractions, and then lyophilized. MS analyses were performed with a TripleTOF 5600 (AB Sciex) mass spectrometer. The acquired raw data files (wiff) of each fraction were combined to search against the protein database of *S. pneumoniae* D39, and ProteinPilot software 4.5 (AB Sciex) was used to identify and quantify the proteins. The parameters used for mass spectrometry and quantitative analysis were set as follows: sample type, iTRAQ 4plex (peptide labeled); cysteine alkylation, iodoacetic acid; digestion, trypsin; instrument, Triple-TOF 5600; ID focus, biological modifications; database, *S. pneumoniae* D39_fasta; search effort, thorough; and detected protein threshold [unused ProtScore (Conf)], >1.30 (95.0%) (23, 35). The iTRAQ was then used for protein quantification, and peptides with a global false discovery rate of \leq 1% were considered for further analysis. The fold change was calculated as the 116/114 ratio for differentially expressed proteins. In this study, the cutoff threshold for upregulation and downregulation of the differentially expressed proteins were defined using the population statistics applied to the biological replicates reported by Gan et al. (36). The finalized cutoffs for upregulation (>1.5) and downregulation (<0.67) of proteins were used.

KEGG was used for the pathway enrichment analysis of 54 differentially expressed proteins in the "Wu Kong" platform (37, 38). Protein-protein interaction network analysis (score > 0.4) using the STRING (39) database (version 10.5) was performed, and the results were visualized with Cytoscape (v3.5.1) (40). The interaction network was further analyzed using Molecular Complex Detection (MCODE) (41).

Transmission electron microscopy analysis. The D39-WT, D39 Δ *spd1495*, and D39*spd1495*⁺ strains in the exponential growth phase were harvested by centrifugation at 10,000 \times *g* for 5 min at 4°C and washed with 0.01 M PBS for three times. Then, all cell pellets were fixed with 2.5% glutaraldehyde fixative and postfixed in 1% osmium tetroxide for 2 h at 4°C. Subsequently, 2% uranyl acetate was added to dye

the cell pellets for 2 h at room temperature. After the dyeing step, the sample was dehydrated with 50% acetone for 15 min, 70% acetone for 15 min, 90% acetone for 15 min, and twice in 100% acetone for 20 min. All samples were then fixed in epoxy resin and left to polymerize at 37°C for 24 h, 45°C for 24 h, and 60°C for 48 h. Each sample was cut into approximately 50- to 80-nm thin slices and then dyed with 3% uranyl acetate and lead citrate. Finally, the prepared samples were detected using TEM (JEOL 2100F; Japanese Electronics Company).

Determination of uronic acid content. The D39-WT, D39 Δ *spd1495*, and D39*spd1495*⁺ strains in the exponential growth phase were harvested by centrifugation at 8,000 \times *g* for 10 min at 4°C and washed with 0.01 M PBS three times. Next, the bacteria were resuspended in Tris-HCl/MgSO₄ buffer (Genebase and Sigma, USA) and centrifuged at 8,000 \times *g* for 5 min at 4°C to remove the supernatant and then resuspended with 500 μ l of Tris-HCl/MgSO₄ buffer again. Next, 200 μ l of bacterial solution and 1.2 ml of 12.5 mM tetraborate solution were mixed and heated at 100°C for 5 min. All of the samples were placed in ice water, and 20 μ l of 15% *m*-hydroxybiphenyl solution was added to each sample, followed by thorough mixing. Meanwhile, the same volume 0.5% NaOH was added in control group. Finally, the concentration of each sample was detected in UV-visible spectroscopy reader at 520 nm (42–44). All of the experimental results were processed by GraphPad Prism 6.0.

Real-time quantitative PCR. For D39-WT and D39 Δ *spd1495*, total RNA was extracted with TRIzol reagent (Invitrogen) according to the manufacturer's protocol following treatment with 100 mg/ml lysozyme. The RNA concentration was determined by using a NanoDrop 2000 UV-VIS spectrophotometer (Thermo Fisher Scientific). A 1- μ g mRNA sample was reverse transcribed using a transScript one-step gDNA removal and cDNA synthesis SuperMix kit for qPCR (TransGen Biotech, China) according to the manufacturer's instructions. RT-qPCR was performed using the StepOne system (Applied Biosystems, USA) with the TransStart Tip Green qPCR supermix kit (TransGen Biotech); 16S RNA was used as an internal control. The cycle threshold (*C_t*) value was recorded, and the relative quantification of gene expression was calculated using the 2^{- $\Delta\Delta$ CT} method (45). The results are presented as the gene expressions in the *spd1495* mutant against those in the D39-WT strain. All data were obtained from three independent biological experiments. The primers used for RT-qPCR are shown in Table 4.

Animal experiments. All of the animals used in this study were purchased from the Department of Experimental Animal (Beijing HFK Bioscience); animal experiments were approved by the Ethics Committee for Animal Experiments of Jinan University. The 6- to 8-week-old female BALB/c mice were cared for according to the institutional guidelines for animal care under standard conditions.

For mouse infections, D39-WT, D39 Δ *spd1495*, and D39*spd1495*⁺ mutants were grown in THY medium and harvested in the exponential growth phase. The bacteria were resuspended in 0.01 M PBS and adjusted to the concentration of 1 \times 10⁷ CFU/50 μ l. Then, 50- μ l portions of the D39-WT, D39 Δ *spd1495*, and D39*spd1495*⁺ strains were injected into 6- to 8-week-old female BALB/c mice (*n* = 8) via tail vein injection. The survival of the mice was recorded every 12 h for 4 days.

Coimmunoprecipitation assay. D39-WT in the exponential growth phase was harvested by centrifugation at 10,000 \times *g* for 10 min at 4°C and washed three times with 0.01 M PBS. D39-WT was resuspended in fresh cell lysates (1 mM phenylmethylsulfonyl fluoride, 50 mM Tris HCl [pH 8.0], 150 mM NaCl, 1% NP-40) until the cell lysates were fully dissolved. The supernatant was collected by centrifugation at 10,000 \times *g* for 10 min at 4°C and then incubated with 40 μ l of protein A/G-agarose (GE Healthcare, USA) and 5 μ l of anti-mouse IgG for 1 h at 4°C, respectively, to remove the nonspecific binding protein, which can bind to IgG, followed by centrifugation at 2,500 \times *g* for 5 min at 4°C. Protein A/G-agarose was added, and the supernatants were incubated again. After centrifugation, the concentrations of supernatants were measured by a BCA protein assay kit. SPD_1495 antibody (2 μ g) and IgG (2 μ g) were added to the supernatants, followed by incubation for 16 h at 4°C, respectively. Then, 40 μ l of protein A/G-agarose was added to bind the proteins at 4°C for 6 h, which were collected by centrifugation at 2,500 \times *g* for 5 min at 4°C and then resuspended in 800- μ l portions of lysates. The isolated proteins were separated by SDS-PAGE, was stained by AgNO₃, and then digested and identified by mass spectrometry (LTQ Orbitrap XL; Thermo Fisher Scientific).

Surface plasmon resonance. For SPR analysis, SPD_1495 protein (30 μ g/ml) was fixed on a NanoGold-COOH sensor chip by capture coupling, and then recombinant ComE and ComE^{D58E} in 0.01 M PBS running buffer were injected sequentially into the chamber at different concentrations (50, 100, 200, and 400 nmol/liter for ComE and 100, 200, 400, 800, and 1,600 nmol/liter for ComE^{D58E}). The interaction of SPD_1495 with ComE was detected by using Open-SPR (Nicoya, Canada) at 25°C. The binding time and disassociation time were both 300 s, the flow rate was 20 μ l/s, and the chip was regenerated with hydrochloric acid (pH 2.5). A one-to-one diffusion-corrected model was fitted to the wavelength shifts corresponding to the various protein concentrations. The data were retrieved and analyzed by using TraceDrawer software.

Electrophoretic mobility shift assay. For EMSA, the 218-bp upstream promoter region of the *cps* gene cluster was amplified by PCR (for the primers, see Table 4) to produce the 5'-biotin-labeled probe Bio-*cps* from D39-WT genomic DNA. The amplified fragment was purified by gel extraction. EMSA was carried out according to the LightShift R chemiluminescent EMSA kit protocol (Thermo Fisher Scientific). Proteins of interest (2, 4, 6, or 8 μ g) and 100 ng of labeled probe were incubated at 37°C for 30 min in 20 μ l of reaction buffer, including 1 \times binding buffer, 1 μ g of poly(dI-dC), 2.5% glycerol, 0.05% NP-40, and 5 mM MgCl₂; the *cps* without binding protein was used as a negative control. After incubation, electrophoresis in 6% native Tris-borate-EDTA polyacrylamide gels was performed at 100 V for 60 min to analyze the binding reactions. The polyacrylamide gels were transferred to nylon membranes at 380 mA for 40 min. The membranes were cross-linked for 10 min using a UV lamp equipped with 254-nm bulbs,

and subsequently biotin-labeled DNA was detected by chemiluminescence according to supplier's instructions (Thermo Fisher Scientific).

Evolutionary analysis. The amino acid sequence of SPD_1495 from *S. pneumoniae* D39 was used to query the NCBI database using the protein BLAST tool. The multiple sequence alignment and cluster analysis of the high-scoring proteins were performed by the software package Clustal-X 2.1. MEGA5.05 was applied to construct the protein evolutionary tree.

Statistics. Data were analyzed by two-tailed, unpaired Student *t* tests, and are expressed as means \pm the standard deviations (SD). Statistical analysis was conducted using Prism 6.0 (GraphPad Software, USA). Results were considered significant at $P < 0.05$.

Data availability. The raw proteomic data and search results have been deposited to the ProteomeXchange Consortium via the PRIDE (46) partner repository and can be accessed with the reviewer account (website, <http://www.ebi.ac.uk/pride>; username, reviewer70538@ebi.ac.uk; password, x5Zecn7h).

SUPPLEMENTAL MATERIAL

Supplemental material is available online only.

TABLE S1, PDF file, 0.02 MB.

ACKNOWLEDGMENTS

This study was supported by the National Natural Science Foundation of China (21977037 to X.S.; 21771199 to R.G.), the National Key R&D Program of China (2017YFA0505100 to Q.-Y.H.), and a Guangzhou Science and Technology Grant (201607010228 to X.S.).

X.S., R.G., and Q.-Y.H. designed the project and revised the paper. Y.-D.Z., Y.P., K.H., and G.-F.D. performed the experiment and data-analysis. Y.-D.Z. and X.S. wrote the manuscript.

REFERENCES

- Drijckoning J, Rohde G. 2014. Pneumococcal infection in adults: burden of disease. *Clin Microbiol Infect* 20:45–51. <https://doi.org/10.1111/1469-0691.12461>.
- World Health Organization. 2007. Pneumococcal conjugate vaccine for childhood immunization: WHO position paper. *Wkly Epidemiol Rec* 82: 93–104.
- O'Brien KL, Hib and Pneumococcal Global Burden of Disease Study Team, Wolfson LJ, Watt JP, Henkle E, Deloria-Knoll M, McCall N, Lee E, Mulholland K, Levine OS, Cherian T. 2009. Burden of disease caused by *Streptococcus pneumoniae* in children younger than 5 years: global estimates. *Lancet* 374:893–902. [https://doi.org/10.1016/S0140-6736\(09\)61204-6](https://doi.org/10.1016/S0140-6736(09)61204-6).
- Abeyta M, Hardy GG, Yother J. 2003. Genetic alteration of capsule type but not PspA type affects accessibility of surface-bound complement and surface antigens of *Streptococcus pneumoniae*. *Infect Immun* 71: 218–225. <https://doi.org/10.1128/iai.71.1.218-225.2003>.
- Ogunniyi AD, Giammarinaro P, Paton JC. 2002. The genes encoding virulence-associated proteins and the capsule of *Streptococcus pneumoniae* are upregulated and differentially expressed *in vivo*. *Microbiology* 148:2045–2053. <https://doi.org/10.1099/00221287-148-7-2045>.
- Kadioglu A, Weiser JN, Paton JC, Andrew PW. 2008. The role of *Streptococcus pneumoniae* virulence factors in host respiratory colonization and disease. *Nat Rev Microbiol* 6:288–301. <https://doi.org/10.1038/nrmicro1871>.
- Guildolin A, Morona J, Morona R, Hansman D, Paton J. 1995. Nucleotide sequence analysis of genes essential for production of *Streptococcus pneumoniae* type 19F capsular polysaccharide. *Dev Biol Stand* 85:267–271.
- Ogunniyi AD, Giammarinaro P, Paton JC. 2002. The genes encoding virulence-associated proteins and the capsule of *Streptococcus pneumoniae* are upregulated and differentially expressed *in vivo*. *Microbiology* 148:2045–2053. <https://doi.org/10.1099/00221287-148-7-2045>.
- Zheng Y, Zhang X, Wang X, Wang L, Zhang J, Yin Y. 2017. ComE, an essential response regulator, negatively regulates the expression of the capsular polysaccharide locus and attenuates the bacterial virulence in *Streptococcus pneumoniae*. *Front Microbiol* 8:277. <https://doi.org/10.3389/fmicb.2017.00277>.
- Yother J. 2011. Capsules of *Streptococcus pneumoniae* and other bacteria: paradigms for polysaccharide biosynthesis and regulation. *Annu Rev Microbiol* 65:563–581. <https://doi.org/10.1146/annurev.micro.62.081307.162944>.
- Geno KA, Gilbert GL, Song JY, Skovsted IC, Klugman KP, Jones C, Konradsen HB, Nahm MH. 2015. Pneumococcal capsules and their types: past, present, and future. *Clin Microbiol Rev* 28:871–899. <https://doi.org/10.1128/CMR.00024-15>.
- Wen Z, Liu Y, Qu F, Zhang JR. 2016. Allelic variation of the capsule promoter diversifies encapsulation and virulence in *Streptococcus pneumoniae*. *Sci Rep* 6:30176. <https://doi.org/10.1038/srep30176>.
- Aanensen DM, Mavroidi A, Bentley SD, Reeves PR, Spratt BG. 2007. Predicted functions and linkage specificities of the products of the *Streptococcus pneumoniae* capsular biosynthetic loci. *J Bacteriol* 189: 7856–7876. <https://doi.org/10.1128/JB.00837-07>.
- James DB, Gupta K, Hauser J, Yother J. 2013. Biochemical activities of *Streptococcus pneumoniae* serotype 2 capsular glycosyltransferases and significance of suppressor mutations occurring in the initiating glycosyltransferase Cps2E. *J Bacteriol* 195:e00715-13. <https://doi.org/10.1128/JB.00715-13>.
- Iannelli F, Pearce BJ, Pozzi G. 1999. The type 2 capsule locus of *Streptococcus pneumoniae*. *J Bacteriol* 181:2652–2654. <https://doi.org/10.1128/JB.181.8.2652-2654.1999>.
- Giammarinaro P, Paton JC. 2002. Role of RegM, a homologue of the catabolite repressor protein CcpA, in the virulence of *Streptococcus pneumoniae*. *Infect Immun* 70:5454–5461. <https://doi.org/10.1128/iai.70.10.5454-5461.2002>.
- Luo P, Morrison DA. 2003. Transient association of an alternative sigma factor, ComX, with RNA polymerase during the period of competence for genetic transformation in *Streptococcus pneumoniae*. *J Bacteriol* 185: 349–358. <https://doi.org/10.1128/jb.185.1.349-358.2003>.
- Reyes A, Leiva A, Cambiazo V, Méndez MA, Gonzalez M. 2006. Cop-like operon: structure and organization in species of the *Lactobacillales* order. *Biol Res* 39:87–93. <https://doi.org/10.4067/s0716-97602006000100010>.
- Wu K, Xu H, Zheng Y, Wang L, Zhang X, Yin Y. 2016. CpsR, a GntR family regulator, transcriptionally regulates capsular polysaccharide biosynthesis and governs bacterial virulence in *Streptococcus pneumoniae*. *Sci Rep* 6:29255. <https://doi.org/10.1038/srep29255>.
- Kloosterman TG, Hendriksen WT, Bijlsma JJ, Bootsma HJ, van Hijum SA, Kok J, Hermans PW, Kuipers OP. 2006. Regulation of glutamine and glutamate metabolism by GlnR and GlnA in *Streptococcus pneumoniae*. *J Biol Chem* 281:25097–25109. <https://doi.org/10.1074/jbc.M601661200>.
- Ulijasz AT, Andes DR, Glasner JD, Weisblum B. 2004. Regulation of iron transport in *Streptococcus pneumoniae* by RitR, an orphan response regulator. *J Bacteriol* 186:8123–8136. <https://doi.org/10.1128/JB.186.23.8123-8136.2004>.

22. Brown JS, Gilliland SM, Ruiz-Albert J, Holden DW. 2002. Characterization of Pit, a *Streptococcus pneumoniae* iron uptake ABC transporter. *Infect Immun* 70:4389–4398. <https://doi.org/10.1128/iai.70.8.4389-4398.2002>.
23. Yang XY, He K, Du G, Wu X, Yu G, Pan Y, Zhang G, Sun X, He QY. 2016. Integrated translomics with proteomics to identify novel iron-transporting proteins in *Streptococcus pneumoniae*. *Front Microbiol* 7:78. <https://doi.org/10.3389/fmicb.2016.00078>.
24. Sadykov MR, Mattes TA, Luong TT, Zhu Y, Day SR, Sifri CD, Lee CY, Somerville GA. 2010. Tricarboxylic acid cycle-dependent synthesis of *Staphylococcus aureus* type 5 and 8 capsular polysaccharides. *J Bacteriol* 192:1459–1462. <https://doi.org/10.1128/JB.01377-09>.
25. Hammerschmidt S, Wolff S, Hocke A, Rosseau S, Muller E, Rohde M. 2005. Illustration of pneumococcal polysaccharide capsule during adherence and invasion of epithelial cells. *Infect Immun* 73:4653–4667. <https://doi.org/10.1128/IAI.73.8.4653-4667.2005>.
26. Briles D, Crain M, Gray B, Forman C, Yother J. 1992. Strong association between capsular type and virulence for mice among human isolates of *Streptococcus pneumoniae*. *Infect Immun* 60:111–116. <https://doi.org/10.1128/IAI.60.1.111-116.1992>.
27. Kim JO, Weiser JN. 1998. Association of intrastrain phase variation in quantity of capsular polysaccharide and teichoic acid with the virulence of *Streptococcus pneumoniae*. *J Infect Dis* 177:368–377. <https://doi.org/10.1086/514205>.
28. Dickey SW, Cheung GY, Otto M. 2017. Different drugs for bad bugs: antivirulence strategies in the age of antibiotic resistance. *Nat Rev Drug Discov* 16:457–471. <https://doi.org/10.1038/nrd.2017.23>.
29. Wach A. 1996. PCR-synthesis of marker cassettes with long flanking homology regions for gene disruptions in *S. cerevisiae*. *Yeast* 12:259–265. [https://doi.org/10.1002/\(SICI\)1097-0061\(19960315\)12:3%3C259::AID-YEA901%3E3.0.CO;2-C](https://doi.org/10.1002/(SICI)1097-0061(19960315)12:3%3C259::AID-YEA901%3E3.0.CO;2-C).
30. Bayle L, Chimalapati S, Schoehn G, Brown J, Vernet T, Durmort C. 2011. Zinc uptake by *Streptococcus pneumoniae* depends on both AdcA and AdcAll and is essential for normal bacterial morphology and virulence. *Mol Microbiol* 82:904–916. <https://doi.org/10.1111/j.1365-2958.2011.07862.x>.
31. Biswas I, Jha JK, Fromm N. 2008. Shuttle expression plasmids for genetic studies in *Streptococcus mutans*. *Microbiology* 154:2275–2282. <https://doi.org/10.1099/mic.0.2008/019265-0>.
32. Dai H, Chen J-h, Shen Y, Zhou X-h, Xu Z-z, Chen X, Jiao X-a. 2018. Production of monoclonal antibodies against chicken interleukin-4 and development of a capture enzyme-linked immunosorbent assay. *Pakistan Vet J* 38:286–290.
33. Miao X, He J, Zhang L, Zhao X, Ge R, He QY, Sun X. 2018. A novel iron transporter SPD_1590 in *Streptococcus pneumoniae* contributing to bacterial virulence properties. *Front Microbiol* 9:1624. <https://doi.org/10.3389/fmicb.2018.01624>.
34. Archambaud C, Nahori M-A, Pizarro-Cerda J, Cossart P, Dussurget O. 2006. Control of *Listeria* superoxide dismutase by phosphorylation. *J Biol Chem* 281:31812–31822. <https://doi.org/10.1074/jbc.M606249200>.
35. Yang X-Y, Shi T, Du G, Liu W, Yin X-F, Sun X, Pan Y, He Q-Y. 2016. iTRAQ-based proteomics revealed the bactericidal mechanism of sodium New Houttuynonate against *Streptococcus pneumoniae*. *J Agric Food Chem* 64:6375–6382. <https://doi.org/10.1021/acs.jafc.6b02147>.
36. Gan CS, Chong PK, Pham TK, Wright PC. 2007. Technical, experimental, and biological variations in isobaric tags for relative and absolute quantitation (iTRAQ). *J Proteome Res* 6:821–827. <https://doi.org/10.1021/pr060474i>.
37. Bateman A, Coin L, Durbin R, Finn RD, Hollich V, Griffiths-Jones S, Khanna A, Marshall M, Moxon S, Sonnhammer ELL, Studholme DJ, Yeats C, Eddy SR. 2004. The Pfam protein families database. *Nucleic Acids Res* 32:D138–D141. <https://doi.org/10.1093/nar/gkh121>.
38. Finn RD, Coghill P, Eberhardt RY, Eddy SR, Mistry J, Mitchell AL, Potter SC, Punta M, Qureshi M, Sangrador-Vegas A, Salazar GA, Tate J, Bateman A. 2016. The Pfam protein families database: towards a more sustainable future. *Nucleic Acids Res* 44:D279–D285. <https://doi.org/10.1093/nar/gkv1344>.
39. Szklarczyk D, Morris JH, Cook H, Kuhn M, Wyder S, Simonovic M, Santos A, Doncheva NT, Roth A, Bork P, Jensen LJ, von Mering C. 2017. The STRING database in 2017: quality-controlled protein-protein association networks, made broadly accessible. *Nucleic Acids Res* 45:D362–D368. <https://doi.org/10.1093/nar/gkw937>.
40. Shannon P, Markiel A, Ozier O, Baliga NS, Wang JT, Ramage D, Amin N, Schwikowski B, Ideker T. 2003. Cytoscape: a software environment for integrated models of biomolecular interaction networks. *Genome Res* 13:2498–2504. <https://doi.org/10.1101/gr.1239303>.
41. Bader GD, Hogue CW. 2003. An automated method for finding molecular complexes in large protein interaction networks. *BMC Bioinformatics* 4:2. <https://doi.org/10.1186/1471-2105-4-2>.
42. Sørensen UBS, Henriksen J, Chen H-C, Szu SC. 1990. Covalent linkage between the capsular polysaccharide and the cell wall peptidoglycan of *Streptococcus pneumoniae* revealed by immunochemical methods. *Microb Pathog* 8:325–334. [https://doi.org/10.1016/0882-4010\(90\)90091-4](https://doi.org/10.1016/0882-4010(90)90091-4).
43. Morona JK, Morona R, Paton JC. 2006. Attachment of capsular polysaccharide to the cell wall of *Streptococcus pneumoniae* type 2 is required for invasive disease. *Proc Natl Acad Sci U S A* 103:8505–8510. <https://doi.org/10.1073/pnas.0602148103>.
44. Trappetti C, McAllister LJ, Chen A, Wang H, Paton AW, Oggioni MR, McDevitt CA, Paton JC. 2017. Autoinducer 2 signaling via the phosphotransferase FruA drives galactose utilization by *Streptococcus pneumoniae*, resulting in hypervirulence. *mBio* 8:e02269-16. <https://doi.org/10.1128/mBio.02269-16>.
45. Xiao-Yan Y, Li N, Xu J-Y, Sun X, He Q-Y. 2019. Lipoprotein SPD_1609 of *Streptococcus pneumoniae* promotes adherence and invasion to epithelial cells contributing to bacterial virulence. *Front Microbiol* 10:1769. <https://doi.org/10.3389/fmicb.2019.01769>.
46. Vizcaíno JA, Csordas A, del-Toro N, Dienes JA, Griss J, Lavidas I, Mayer G, Perez-Riverol Y, Reisinger F, Ternent T, Xu Q-W, Wang R, Hermjakob H. 2016. 2016 update of the PRIDE database and its related tools. *Nucleic Acids Res* 44:D447–D456. <https://doi.org/10.1093/nar/gkv1145>.